PHYSICAL REVIEW B VOLUME 15, NUMBER 4 15 FEBRUARY 1977

Crystal field and magnetic properties in some cubic holmium compounds

D. Schmitt, P. Morin, and J. Pierre
Laboratoire de Magnétisme, Centre National de la Recherche Scientifique, 166X, 38042-Grenoble-Cedex, France
(Received 3 May 1976)

Crystal-field parameters have been determined by neutron spectroscopy on some holmium intermetallic compounds of CsCl structure (HoCu, HoAg, HoZn, HoMg). The variation of parameters with the alloyed metal is very similar to the results previously observed on isomorphous erbium compounds. The behavior of $A_4\langle r^4\rangle$ seems to reflect the influence of d electrons of the alloyed metal. The fourth-order terms present a significant shift between Ho and Er series, whereas the sixth-order ones always remain of the same order of magnitude. We discuss the influence of these parameters on the magnetic properties in the ordered state.

I. INTRODUCTION

Numerous studies have been undertaken on rare-earth intermetallic compounds in order to determine the crystalline electric field (CEF) parameters.[1,2] In most cases, the point-charge model — even modified by evaluating the ligand effective charges from band calculations — is inadequate to explain the experimental results. On the other hand the importance of $4f$-shell–conduction-band coupling has been shown, giving rise to Coulombic and exchange contributions to the crystal field.[3-5]

It is interesting to study the variations of CEF parameters in isomorphous series where the rare-earth or the alloyed metal can be substituted:

(i) The charge distribution of the rare-earth ion influences the Coulombic term — mostly through the radial expansion in the $A_n\langle r^n\rangle$ parameters — and the exchange term in a much more complex manner. Such a variation has been revealed for instance in the study of rare earths diluted in noble metals[6] or yttrium[7].

(ii) The CEF parameters vary as a function of the valency of the alloyed metal, of the electron transfer related to the electronegativity difference, and the angular distribution of conduction electrons.

Such systematic studies have been undertaken, for instance in RM compounds (M = N, P, As, Sb, Bi...) with NaCl structure[8] or RM_3 compounds, M = Sn, Pb, In, with $AuCu_3$ structure.[9] We have studied in previous papers the behavior of ErM compounds (M = Cu, Ag, Zn,[10] Pd, and[11] Mg) by neutron spectroscopy. The study in rare-earth series has been undertaken for RRh compounds by the same technique[12] and for RZn compounds by anisotropy measurements on single crystals.[13]

We present in this paper an investigation by neutron spectroscopy of HoM compounds (M = Cu, Ag, Zn, Mg) together with an interpretation of their magnetic properties.

The sixth-order CEF parameters $A_6\langle r^6\rangle$ for Ho compounds are found close to corresponding ones for Er compounds, but the fourth-order ones $A_4\langle r^4\rangle$ are shifted toward more positive values, the differences ranging from 14 K (Ag) to 40 K (Mg). For HoZn, the experimental parameters do not give an adequate description of the magnetic properties within a molecular-field model with Heisenberg-type exchange; we discuss the possible influence of anisotropic exchange and magnetoelastic couplings.

II. EXPERIMENTAL METHODS

As in previous studies,[10] we have diluted holmium in yttrium in order to lower the magnetic interactions and to study the compound in the paramagnetic state at a temperature where the ground level only is populated. The compounds studied were $Ho_{0.25}Y_{0.75}Cu$, $Ho_{0.2}Y_{0.8}Ag$, $Ho_{0.2}Y_{0.8}Mg$, and $Ho_{0.15}Y_{0.85}Zn$. They were prepared by melting the constituents — in sealed tantalum crucibles for the two last ones — and quenching the melt. The holmium concentration was chosen lower for Zn compound due to larger interactions, and higher for Cu compound because pure YCu undergoes a crystallographic change at low temperature.

The neutron spectroscopy experiments were performed as previously on the time-of-flight spectrometer IN7 at the Institut Laue-Langevin high flux reactor of Grenoble. The time-of-flight basis was reduced to 2.35 m instead of 4 m, which increases the intensity and does not greatly affect the resolution.

III. NEUTRON SPECTROSCOPY RESULTS

The results were analyzed within the classical formalism; the CEF Hamiltonian is written as[14]

$$\mathcal{H}_c = WxO_4/F_4 + W(1-|x|)O_6/F_6$$
$$= A_4\beta\langle r^4\rangle O_4 + A_6\gamma\langle r^6\rangle O_6$$

and leads to the level scheme of Fig. 1 for the trivalent holmium ion (J = 8).

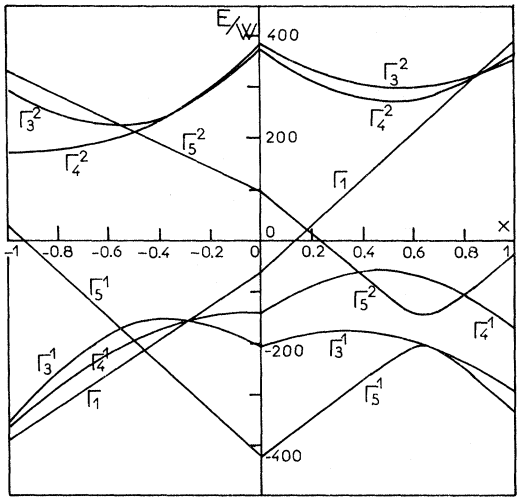

FIG. 1. Crystal-field energy levels for $J=8$ as a function of x (Ref. 14).

The theoretical aspects were quoted in previous papers.[10,11] Calculations are based on the neutron cross section derived by Trammell,[15] where the intensities of transitions are related to the matrix elements between levels.[16] Due to the number of possible transitions in the case of Ho^{3+}, theoretical fits are necessary to describe both positions and intensities of inelastic lines. In these fits, besides the CEF parameters, the elastic peak intensity, the spectrometer resolution, and natural transition widths must be taken into account.

The spectrometer resolution is a constant in time-of-flight and thus depends on incident energy E_0 (it is about 1.5 meV for $E_0=20$ meV). This is verified on the full width at half maximum of the elastic lines. The observed widths for inelastic lines are generally slightly larger; assuming Gaussian shapes, we may deduce that natural transition widths are in the range 0.5–1.5 meV, that is smaller than in previous studies. One major contribution to linewidths at low temperatures is certainly exchange broadening, as can be seen on the most concentrated compound $Ho_{0.25}Y_{0.75}Cu$ for $E_0=6.65$ meV (Fig. 2). This contribution within each representation may also lead to a broadening of the quasielastic line, in addition to nuclear incoherent scattering and to the scattering from the cryostat and sample holder. At higher temperatures, an additional term arises from ion-phonon coupling. For sake of simplicity, all the fits are drawn with a constant natural width of 0.5 meV.

Two spectra are given for each compound: the spectrum performed at low temperature shows mainly excitations from the ground state and leads to a first determination of the level scheme; at higher temperature the spectrum allows one to check this scheme by the appearance of new transitions from excited levels in both energy-gain and energy-loss processes, and by the variation of lines intensities according to the Boltzmann factors.

In $Ho_{0.25}Y_{0.75}Cu$ compound (Fig. 2), the CEF

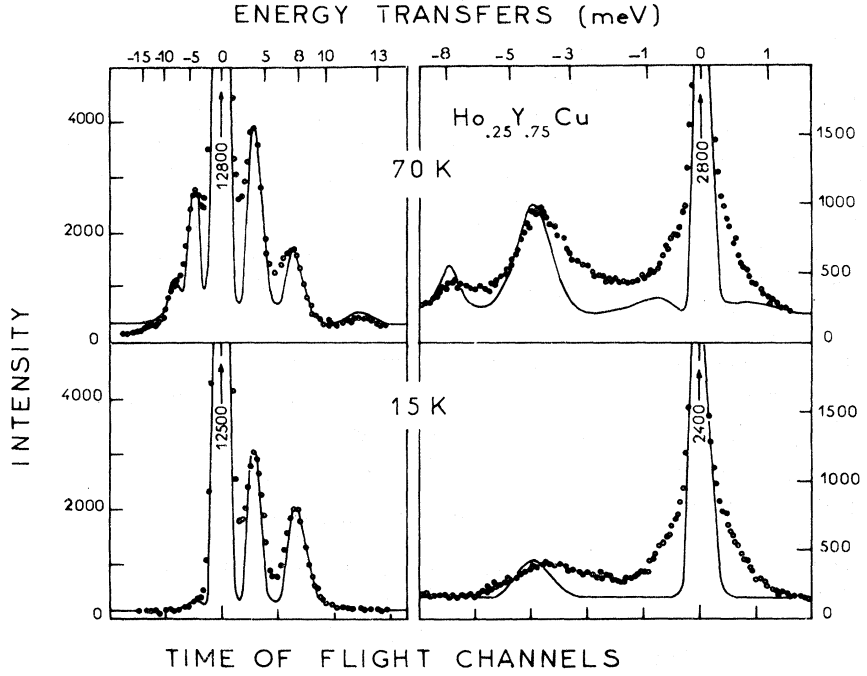

FIG. 2. Time-of-flight spectra for $Ho_{0.25}Y_{0.75}Cu$ at 15 and 70 K. The left-hand side spectra are relative to an incident energy $E_0=26.6$ meV, the right-hand side ones to $E_0=6.65$ meV. Solid lines are theoretical fits.

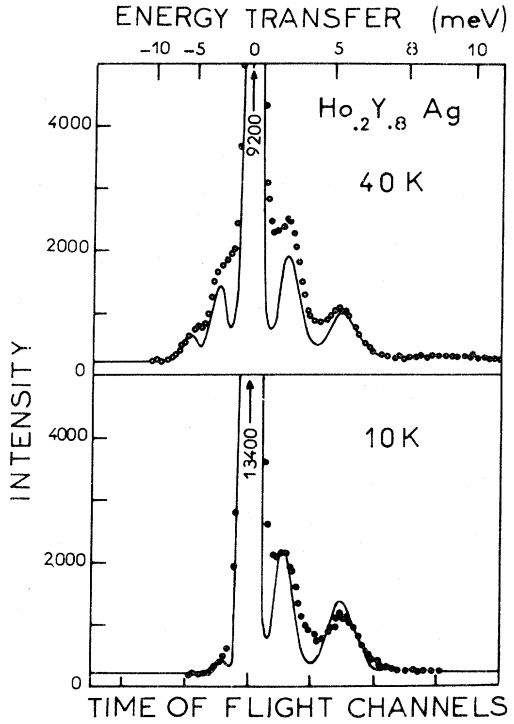

FIG. 3. Time-of-flight spectra for $Ho_{0.2}Y_{0.8}Ag$ at 10 and 40 K. The incident energy is $E_0 = 19.39$ meV. Solid lines are theoretical fits.

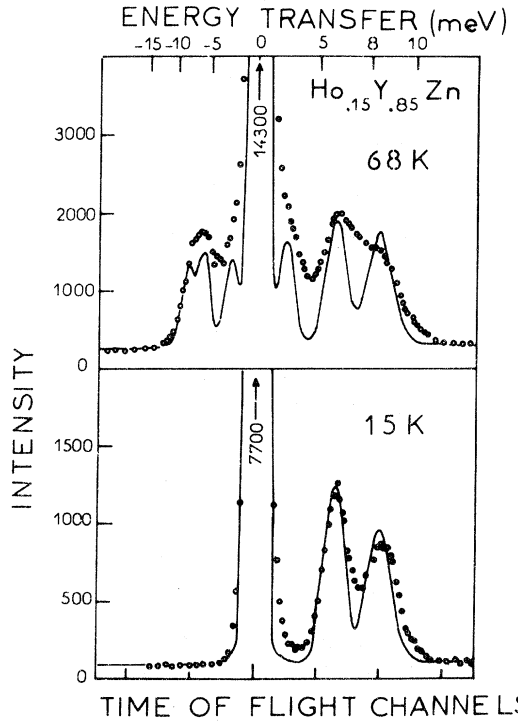

FIG. 4. Time-of-flight spectra for $Ho_{0.15}Y_{0.85}Zn$ at 15 and 68 K ($E_0 = 22.69$ meV). Solid lines are theoretical fits.

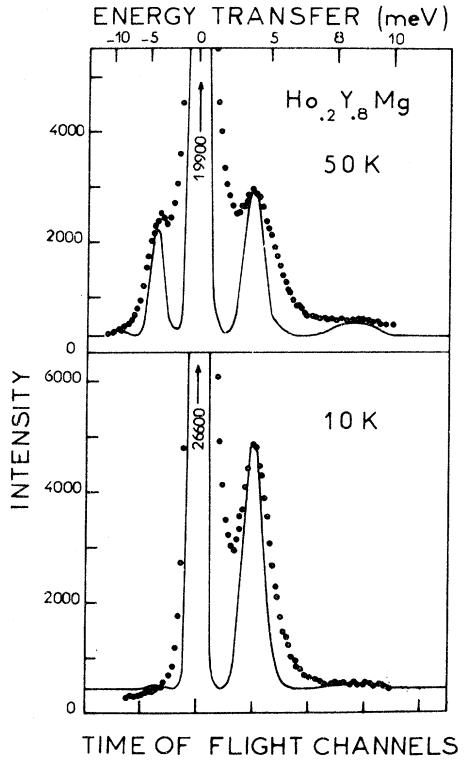

FIG. 5. Time-of-flight spectra for $Ho_{0.2}Y_{0.8}Mg$ at 10 and 50 K ($E_0 = 19.39$ meV). Solid lines are theoretical fits.

scheme is determined without ambiguity with parameters $W = 0.40 \pm 0.02$ K (0.0345 meV); $x = 0.34 \pm 0.02$. The two transitions observed at 15 K, for an incident energy $E_0 = 26.6$ meV, connect the Γ_5^1 ground level to the Γ_3^1 and Γ_4^1 levels (Fig. 6). The third transition near 12 meV observed at 70 K connects, respectively, Γ_4^1 to Γ_4^2 and Γ_5^2 to Γ_3^2 levels. With an incident energy of 6.65 meV (first-order reflection on the copper monochromator), the two first transitions were also recorded as deexcitation processes.

In $Ho_{0.2}Y_{0.8}Ag$ compound (Fig. 3), the incident energy was lowered to $E_0 = 19.39$ meV. The two observed transitions may be encountered for $W > 0$ at $x = 0.42$ or 0.58; however the intensity ratio tends to rule out the second solution. The CEF parameters thus obtained are $W = 0.32 \pm 0.02$ K, $x = 0.42 \pm 0.02$ in perfect agreement with a determination by Tellenbach *et al.*[17]

In $Ho_{0.15}Y_{0.85}Zn$ compound (Fig. 4), the best agreement is obtained with $W = 0.36 \pm 0.02$ K and $x = 0.08 \pm 0.02$. The fit at 68 K could be improved by taking slightly different parameters.

In $Ho_{0.2}Y_{0.8}Mg$ compound (Fig. 5), only one intense transition is observed. Such a situation can be encountered only for $W > 0$ and $x \sim -0.3$, when

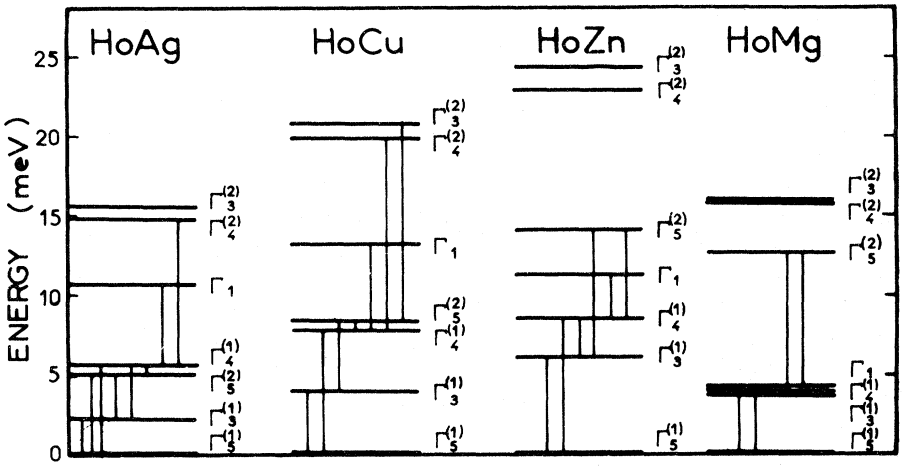

FIG. 6. Level schemes in HoM compounds. Vertical lines correspond to the observed transitions.

the three levels Γ_3^1, Γ_4^1, Γ_1 are close (Fig. 6). Another possibility with $x \sim 0.8$ is ruled out by the occurrence of the weak transition at 8.6 meV and the magnetization anisotropy observed in strong field (see Sec. V). The best agreement is obtained for $W = 0.32 \pm 0.02$ K; $x = -0.26 \pm 0.04$.

The level schemes obtained for each compound from the theoretical fits are given on the Fig. 6, as well as the transitions which contribute noticeably to the spectra.

IV. ANALYSIS OF CRYSTAL-FIELD PARAMETERS

The values of CEF parameters W, x, $A_4\langle r^4\rangle$, $A_6\langle r^6\rangle$ determined in holmium compounds are given in Table I. The variation of parameters is very similar to that in erbium series[10,11]; however, there exists a significant positive shift for the $A_4\langle r^4\rangle$ parameter in Ho compounds.

$A_4\langle r^4\rangle$ increases continuously from a negative value with the number of outer electrons on the alloyed metals, through the sequence Rh, Pd, Ag and Cu, Zn and Mg. It changes its sign for this last element; its magnitude for isoelectronic compounds does not seem to be correlated with the lattice parameter a. The sixth-order term remains negative and of the same order of magnitude; however, its amplitude decreases with a, but differs from the a^{-7} law as expected in the point-charge model. This very different behavior can indicate different origins for both terms.

In order to analyze the CEF parameters varia-

TABLE I. Magnetic data, lattice parameter, and crystal-field parameters in holmium and erbium compounds.[a]

	HoRh (Ref. 12)	HoCu	HoAg	HoZn	HoMg
T_{order} (K)	3.2 AF	28 AF	33 AF	75 F	21 NC
μ_{obs} (μ_B)	5.2 ±0.3	8.35 ±0.40	8.0 ±0.2	8.45 ±0.05	> 5
a(Å) at 300 K	3.377	3.444	3.593	3.547	3.761
W (K)	0.58	0.40	0.32	0.36	0.32
x	0.43	0.34	0.42	0.08	−0.26
$A_4\langle r^4\rangle$ (K)	−125 ±19	−68 ±8	−67 ±7	−14 ±4	+42 ±9
$A_6\langle r^6\rangle$ (K)	−18 ±3	−15 ±1	−12 ±1	−18 ±1	−13 ±1
	ErRh (Ref. 12)	ErCu (Ref. 10)	ErAg (Ref. 10)	ErZn (Ref. 10)	ErMg (Ref. 11)
$A_4\langle r^4\rangle$ (K)	−123 ±10	−84 ±7	−82 ±6	−36 ±5	−4 ±3
$A_6\langle r^6\rangle$ (K)	−19 ±1	−15 ±1	−10 ±1	−18 ±1	−11 ±1

[a]Magnetic structures—AF: antiferromagnet; F: ferromagnet; NC: noncollinear.

tion, the ligand effective charges have been first evaluated starting from augmented-plane-wave calculations[18,19] and taking into account the electron density in these ligands spheres: their contribution is always small, less than 10 K for $A_4\langle r^4\rangle$ and about -1 K for $A_6\langle r^6\rangle$.

The major contribution to $A_4\langle r^4\rangle$ arises from the d electrons of the conduction band and the variation of the CEF parameters reflects the progressive localization of the d electrons of the alloyed metal, which leads to a spatial redistribution in the rare-earth sphere. From augmented-plane-wave results on YMg,[18] and DyRh,[19] we have derived the Coulombic contribution of the d electrons inside the central rare-earth sphere from their spatial distribution and the $4f$ radial wave functions.[20] We have obtained $(A_4\langle r^4\rangle)_{\text{Coulomb}} = +30$ K for DyRh and +150 K for DyMg. This gives the order of magnitude for the Coulombic contribution in a series with a given alloyed metal. Inside a series, this value is expected to vary mostly through the radial expansion $\langle r^4\rangle$, while the band does not change much: the $\langle r^4\rangle$ difference of 8% between Ho^{3+} and Er^{3+} may thus contribute to a variation of about 3 K in Rh compounds and 15 K in Mg compounds for $(A_4\langle r^4\rangle)_{\text{Coulomb}}$.

The observed variation between Rh and Mg compounds is well reproduced by the calculation of the Coulombic term, but the systematic shift must be ascribed to the occurrence of another contribution with opposite sign, arising for instance from the exchange term of the $4f$ shell with the band as predicted for rare earths diluted in noble metals.[4,6]

The large order of magnitude of the sixth-order term is still unexplained; covalency effects or $4f$ exchange with the conduction band may contribute to this term.

V. MAGNETOCRYSTALLINE ANISOTROPY IN HoM CONCENTRATED COMPOUNDS

A. HoZn compound

The magnetic properties of HoZn have been studied previously by means of magnetic measurements on a spherical single crystal[13] and by specific-heat experiments.[21] The moments order ferromagnetically at $T_c = 75$ K along a threefold axis, but they rotate suddenly at $T_R = 23$ K toward a twofold axis; this first-order transition has been explained as due to the free-energy variations related to the difference of the level-scheme splitting along [110] and [111] quantization axes.

The experimental magnetization curves along the three principal axes are given in Fig. 7, for $T = 4.2$ K, and in the inset for 30 K. An anisotropic reduction of the moment by the CEF is observed. We have calculated the theoretical magnetization when the field is applied along the three principal directions in a molecular-field theory, starting from the CEF level-scheme determined above:

$$\mathcal{H} = \mathcal{H}_{CEF} - g\mu_B(\vec{H}_{ex} + \vec{H}_i)\cdot\vec{J}.$$

H_i is the internal field, the exchange field H_{ex} being taken as $H_{ex} = ng\mu_B\langle J_z\rangle_T$ with the molecular-

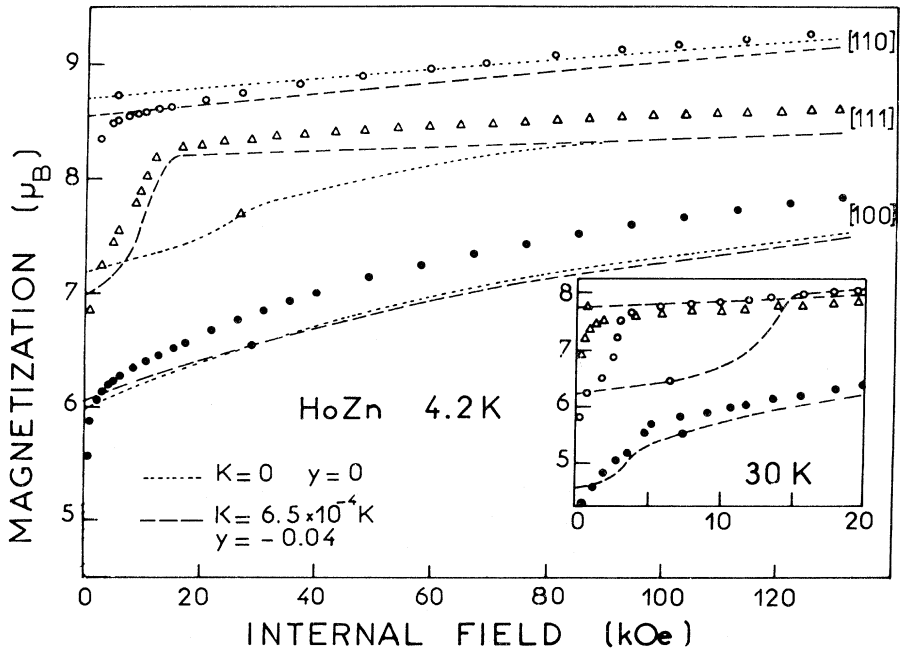

FIG. 7. Magnetization curves for a monocrystalline HoZn sample at 4.2 K (and 30 K for inset). Dotted curves are calculated with $W = 0.36$ K, $x = 0.08$; hatched curves are obtained by adding biquadratic exchange and magnetoelastic terms. To avoid confusion, the axes symbols are repeated once on the theoretical curves.

field coefficient $n = T_c/C$. Our calculation performs the diagonalization of the perturbing Hamiltonian in the plane defined by the easy axis and the field direction, that allows one to describe the moment rotation toward hard axes. The calculated variations of the magnetization (dotted lines on the Fig. 7) are in rather good agreement at 4.2 K with the experimental ones, although the calculated values are smaller. However, the energy difference between the twofold and threefold axes is computed too large, as can be seen during the rotation of the moment towards the field applied along the threefold axis. Furthermore, the previous Hamiltonian is not able to describe the temperature dependence of magnetic properties: it leads to equal free energies along [110] and [111] at a rotation temperature $T_R = 60$ K, far from the experimental value $T_R = 23$ K. It does not give a very good representation of the temperature dependence for the spontaneous magnetization. This is due in part to the molecular-field formalism which is less satisfactory than the spin-wave model in our RZn compounds.[13]

Different hypotheses may be proposed to improve the preceding model:

(i) First of all, the CEF parameters may change between the diluted paramagnetic system and the concentrated ordered one, if the band structure is modified at the magnetic ordering by the interaction with the $4f$ shell. However, it would be necessary to lessen W by about 50%, or to shift x up to 0.5, to obtain an agreement in high fields.

(ii) Considering an anisotropic exchange contribution, like a biquadratic term, may be not unreasonable. The following expression keeps the cubic symmetry[22]:

$$\mathcal{H}_b = K(\langle O_2^0\rangle_T O_2^0 + 3\langle O_2^2\rangle_T O_2^2).$$

$\langle O_2^0\rangle_T$ and $\langle O_2^2\rangle_T$ are the temperature averages of the corresponding operators in the molecular-field formalism.

(iii) Also, the rhombohedral distortion, observed when the moment points along the threefold axis,[23] gives rise to a second-order term and modifies the fourth- and sixth-order ones. These new terms are difficult to evaluate except for the ligand effective charges contributions. We have only taken into account a second-order term in the magnetoelastic energy, keeping the fourfold axis as quantization axis; it can be written

$$\mathcal{H}_d = Wy(O_2^0 + 2\sqrt{2}\,O_2^1)$$

when the moment lies along [111], y being related to the distortion amplitude.

The influence of these two last contributions, which are often found associated, have been checked on the magnetic properties of HoZn. The biquadratic term is efficient to reduce at low temperatures the anisotropy between the twofold and threefold axes, but due to its rapid thermal decrease, it does not lower enough the rotation temperature. Conversely the introduction of the distortion term alone does not allow us to get simultaneous agreement for the anisotropy at 4.2 K and the rotation temperature. A good description is obtained with both parameters $y = -0.04$ and $K = 6.5 \times 10^{-4}$ K (hatched curves on Fig. 7). We then predict, in agreement with experiments, a rapid increase of the magnetization along [111] axis at 4.2 K and along [110] at 30 K, which reminds of the first-order transition due to the spin rotation at 23 K. As the free energy along the fourfold axis is much higher, the introduction of such terms modifies only slightly the behavior of the magnetization along this axis.

This is not enough to prove the reality or the exact form of such terms, and different experiments will be necessary to check these contributions. Elastic constants measurements have allowed us to separate the magnetoelastic and biquadratic terms in the TmZn and ErZn compounds[24]; preliminary results show that these terms, the first at least, are weak in HoZn. The anisotropy of the magnetoresistivity may reveal the quadrupole coupling of the $4f$ shell with the band, which is one of the possible origins for both contributions.[25]

B. HoCu compound

HoCu orders antiferromagnetically with a propagation vector $\vec{q} = (\frac{1}{2}, \frac{1}{2}, 0)$ (C-type structure) below 28 K. Neutron diffraction leads to a moment value of $(8.35 \pm 0.4)\mu_B$ at 4.2 K and to an angle $\psi = 55°$ between the moment direction and the c axis of the magnetic cell $(2a, 2a, a)$.[26] The moment points along a threefold axis, however, there is some doubt whether the magnetic structure is collinear or not.[27] The susceptibility measured in fields up to 70 kOe does not show any spin flopping phenomenon in the ordered range, but a slight decrease with field. This is opposite to the case of TbCu and ErCu, which have a collinear spin structure and exhibit spin flopping above 20 kOe.

Starting from the level scheme obtained in the paramagnetic state and a value of the exchange field deduced from the ordering temperature, we have looked for the stable direction of the moment. The values of the free energy and of the moment are close along the [110] and [111] axes, the [001] one being clearly the hard direction. Thus the observed structure is well allowed by the level

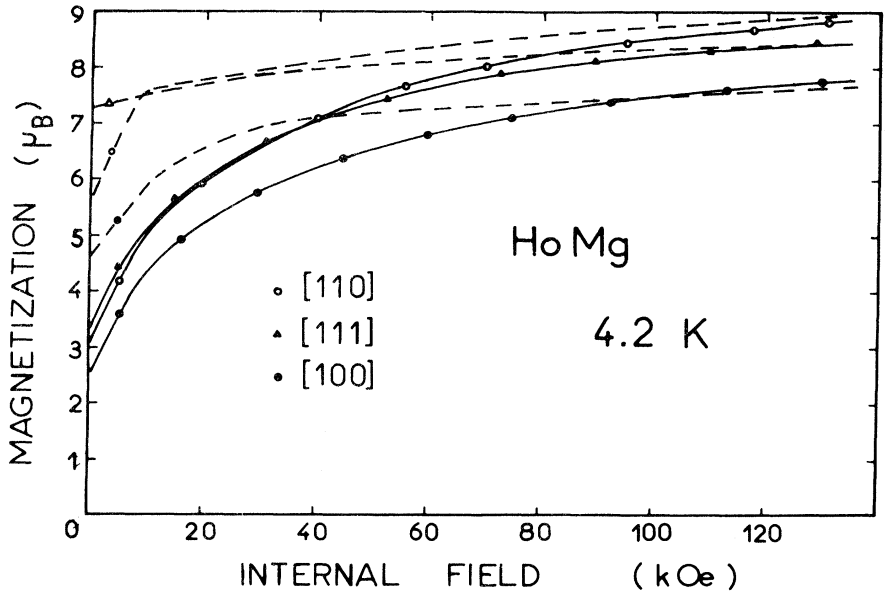

FIG. 8. Magnetization curves for a monocrystalline HoMg sample at 4.2 K. Solid curves are experimental; hatched curves are calculated with $W = 0.32$ K, $x = -0.26$.

scheme; however, the calculated value of the moment ($7.9\mu_B$ with a molecular field of 110 kOe) remains slightly lower than the experimental value.

C. HoAg compound

The compound orders at 33 K. The magnetic structure has been studied by Nereson[28]: he considers an antiferromagnetic structure of C-type, the moment pointing along the c axis ($\psi = 0$), with an amplitude modulation along a fourfold axis perpendicular to the c axis; the maximum value is $(8.0 \pm 0.2)\mu_B$.

The calculation with the determined CEF parameters leads to a small energy difference between [110] and [111] and to a moment value of $8.0\mu_B$ along [110] for a molecular field of 83 kOe, in rough agreement with the Néel temperature. As in the other compounds, the fourfold axis is clearly the hard direction. Thus our calculation suggests the possibility of a multiaxial structure which must correspond to the same diffraction pattern.[27] No distortion was observed in the ordered range by x-ray diffraction, within our experimental resolution (10^{-3}).

Besides, the ground state being a triplet associated with the $\Gamma_5^{(1)}$ representation, the intrinsic moment ($H_{ex} = 0$) is $6.4\mu_B$. Thus, due to entropy considerations, the amplitude-modulated structure described by Nereson should tend at low temperature towards an antiphase structure that is still not observed at 4.5 K. On the other hand, as the magnetocrystalline anisotropy is weak between [110] and [111], the moment direction may rotate from one cell to the other.[32]

D. HoMg compound

Magnetic measurements have been performed on a single crystal of HoMg.[29] It orders at 21 K with a spontaneous magnetization which cannot be defined precisely from our magnetization curves (Fig. 8). Neutron diffraction patterns lead to a ferromagnetic component $\mu_F = (5.0 \pm 0.1)\mu_B$ at 4.2 K. However, the magnetic structure is not simply ferromagnetic, as shown by the low-field behavior of the magnetization and the appearance of diffuse antiferromagnetic reflections on the neutron patterns.[29] With the level scheme, it is possible to calculate the moment value along the three directions as if it was a ferromagnet. The agreement is satisfactory in high magnetic fields (Fig. 8), that proves that the moments are well collinear under such fields, the discrepancies in lower fields being due to the noncollinear structure.

VI. CONCLUSION

The determination of CEF parameters in two series of isomorphous compounds with holmium and erbium has allowed us to discuss the influence of the alloyed metal and the importance of the d electrons in the conduction band. The crystal field being built mainly from Coulombic and exchange terms of large magnitude, which partly cancel each other, small relative variations of these terms may lead to the observed variations between Ho and Er ions.

If the comparison with magnetic properties is

straightforward in the case of a ferromagnet, many more difficulties appear in describing antiferromagnetic ordering, particularly when the neutron diffraction patterns lead to some structure ambiguities. The knowledge of the crystal field then allows one to solve some indeterminations.[30]

ACKNOWLEDGMENTS

We are indebted to Dr. A. Murani for the improvements on the IN7 spectrometer. This work was undertaken with the financial support of the Direction des Recherches et Moyens d 'Essais (Contract No. 75.391).

[1]For a recent review, see Proceedings of the Montréal Conference on Crystal Field in Metals and Alloys, Montréal, 1974, edited by R. A. B. Devine (unpublished).
[2]A. J. Freeman, in *Magnetic Properties of Rare Earth Metals*, edited by R. J. Elliott (Plenum, New York, 1972), Chap. 6, p. 325.
[3]K. C. Das and D. K. Ray, Solid State Commun. 8, 2025 (1970).
[4]H. C. Chow, Phys. Rev. B 7, 3404 (1973).
[5]J. M. Dixon and R. Dupree, J. Phys. F 1, 539 (1971).
[6]G. Williams and L. Hirst, Phys. Rev. 185, 407 (1969).
[7]J. Høg and P. Touborg, Phys. Rev. B 9, 2920 (1974).
[8]R. J. Birgeneau, E. Bucher, J. P. Maita, L. Passell, and K. C. Turberfield, Phys. Rev. B 8, 5345 (1973).
[9]P. Lethuillier and J. Chaussy, J. Phys. 37, 123 (1976).
[10]P. Morin, J. Pierre, J. Rossat-Mignod, K. Knorr, and W. Drexel, Phys. Rev. B 9, 4932 (1974).
[11]P. Morin, J. Pierre, D. Schmitt, and W. Drexel, J. Phys. 37, 611 (1976).
[12]R. Chamard-Bois, J. Rossat-Mignod, K. Knorr, and W. Drexel, Solid State Commun. 13, 1549 (1973); R. Chamard-Bois, J. Rossat-Mignod, K. Knorr, W. Drexel, P. Morin, and J. Pierre, in Ref. 1, p. 65.
[13]R. Aleonard, P. Morin, J. Pierre, Colloq. Int. Cent. Natl. Rech. Sci. 39, C242 (1974); P. Morin, J. Pierre, Phys. Status Solidi A 30, 549 (1975).
[14]K. R. Lea, J. M. Leask, and W. P. Wolf, J. Phys. Chem. Solids 23, 1381 (1962).
[15]G. T. Trammell, Phys. Rev. 92, 1387 (1953).
[16]R. J. Birgeneau, J. Phys. Chem. Solids 33, 59 (1972).
[17]U. Tellenbach, A. Furrer, and A. H. Millhouse, J. Phys. C 8, 3833 (1975).
[18]D. Schmitt, J. Pierre, and M. Belakhovsky, J. Phys. F 6, 789 (1976).
[19]M. Belakhovsky, J. Pierre, and D. K. Ray, J. Phys. F 5, 2274 (1975); M. Belakhovsky and D. K. Ray, Phys. Rev. B 12, 3956 (1975).
[20]A. J. Freeman and R. E. Watson, Phys. Rev. 127, 2058 (1962).
[21]P. Morin and J. Pierre, Solid State Commun. 13, 537 (1973); P. Morin, J. Pierre, and J. Chaussy, Phys. Status Solidi A 24, 425 (1974).
[22]J. Sivardière, J. Magn. Magn. Mater. 1, 23 (1975).
[23]J. Laforest, P. Morin, J. Pierre, and J. S. Shah, C. R. Acad. Sci. B 277, 353 (1973).
[24]P. Morin, A. Waintal, B. Lüthi, in Proceedings of the 12th Rare Earth Research Conference, Vail, Colorado, 1976 (unpublished), p. 95.
[25]A. Fert and A. Friederich, AIP Conf. Proc. 20, 466 (1974).
[26]J. Pierre, in *Proceedings of the Eighth Rare Earth Research Conference, Reno, Nevada, 1970* (U.S. Bureau of Mines, Washington, D.C., 1970), p. 1020.
[27]M. Wintenberger and R. Chamard-Bois, Acta Crystallogr. A 28, 341 (1972).
[28]N. Nereson, AIP Conf. Proc. 10, 669 (1972).
[29]R. Aleonard, P. Morin, J. Pierre, and D. Schmitt, J. Phys. F 6, 1361 (1976).
[30]P. Morin and R. de Combarieu, Solid State Commun. 17, 975 (1975).
[31]R. W. Hill, J. Cosier, and D. A. Hukin, J. Phys. F 6, 1731 (1976).
[32]The hyperfine specific heat of HoAg has been recently measured.[31] It is consistent with an unique moment value of $8.6\mu_B$.